Article published online: 2024-10-23

Antimicrobial Effect of Zinc Oxide Nanoparticle Coating on Titanium 6 Aluminum 4 Vanadium (Ti-6Al-4V)-Fixed Orthodontic Retainer Substrate

Shahbaa A. Mohammed[1] Mohammed Nahidh[1] Mohammed K. Khalaf[2] Maria Maddalena Marrapodi[3] Marco Cicciù[4] Giuseppe Minervini[5,6]

[1] Department of Orthodontics, College of Dentistry, University of Baghdad, Baghdad, Iraq
[2] Ministry of Higher Education and Scientific Research/Science and Technology, Baghdad, Iraq
[3] Department of Woman, Child and General and Specialist Surgery, University of Campania "Luigi Vanvitelli", Naples, Italy
[4] Department of Biomedical and Surgical and Biomedical Sciences, Catania University, Catania, Italy
[5] Multidisciplinary Department of Medical-Surgical and Dental Specialties, University of Campania Luigi Vanvitelli, Caserta, Italy
[6] Saveetha Dental College and Hospitals, Saveetha Institute of Medical and Technical Sciences (SIMATS), Saveetha University, Chennai, Tamil Nadu, India

Address for correspondence Maria Maddalena Marrapodi, MD, Department of Woman, Child and General and Specialist Surgery, University of Campania "Luigi Vanvitelli", 80121 Naples, Italy (e-mail: mariamaddalena.marrapodi@studenti.unicampania.it).

Eur J Gen Dent

Abstract

Objectives Due to its excellent biocompatibility, superior mechanical qualities, and exceptional corrosion resistance, titanium 6 aluminum 4 vanadium (Ti-6Al-4V) alloy is frequently used for medical and orthodontic purposes as a fixed retainer after active orthodontic treatment. Titanium lacks the antibacterial characteristics and is bioinert, this may influence the usage of such materials in the field of biomedical applications. Bacterial adhesion to the orthodontic retainer surface is a common first step in infection; this is followed by bacterial colonization ending with the formation of a biofilm. Once biofilm forms, it is highly resistant to medicines and the host immune system's defense mechanism, making it difficult to remove the biofilm from orthodontic retainer. This study aimed to test the antimicrobial effect of a zinc oxide (ZnO) nanoparticle coating on Ti-6Al-4V orthodontic retainers.

Materials and Methods ZnO nanoparticles, with a particle size of 10 to 30 nm, were used to coat the alloy using the electrophoretic deposition method. Various parameters and surface characterization tests were employed to obtain an optimized sample. This sample was subjected to the microbial adherence optical density test to examine the adherence of *Streptococcus mutans*, *Lactobacillus acidophilus* bacteria, and *Candida albicans*.

Results The optimized sample had a 5-mg/L ZnO concentration, applied voltage of 50 V, and a 1-cm distance between electrodes. The ZnO coating significantly reduced microbial adherence compared to uncoated samples, effectively inhibiting bacterial development.

Keyword
- fixed orthodontic retainer
- ZnO nanoparticles
- antimicrobial activity

DOI https://doi.org/10.1055/s-0044-1789242.
ISSN 2320-4753.

Thieme Medical and Scientific Publishers Pvt. Ltd., A-12, 2nd Floor, Sector 2, Noida-201301 UP, India

Conclusion Electrophoretic deposition is an efficient and cost-effective technique for coating orthodontic titanium retainer substrates. Coating Ti-6Al-4V with ZnO nanoparticles increased the antimicrobial effectiveness of the material and as the concentration of the nanoparticles rises, the antimicrobial effect increases too.

Introduction

Electrophoretic deposition (EPD) uses the movement and deposition of charged particles onto a conductive electrode in an electric field to generate thin or thick films and coatings. EPD may be used to process a broad range of powdered or colloidal materials, including metals, ceramics, polymers, and composites. This technique has been used extensively, in particular, to cover metal and alloy implants with ceramic particles.[1]

Metals are used to create several orthodontic materials because of their outstanding mechanical qualities. The coating on the surface of a substance is a crucial factor in determining its usefulness. In recent years, antimicrobial and functional surface coatings have been created.[2]

Metal oxide nanoparticles (NPs) offer the biomedical sector a bright and expansive future, the delivery of drugs and genes to kill germs and cancer cells; cell imaging; biosensing; and other uses.[3]

Zinc oxide NPs (ZnO NPs) are one of the most important metal oxide NPs and find widespread use due to their exceptional physical and chemical properties.[4]

The ZnO NPs have undergone extensive antimicrobial research over the last two decades, and their popularity is a result of their superior antibacterial effect than that of silver and titanium. Monteiro et al have shown that ZnO NPs are deadly to microbial cells but safe for human cells at the same dose.[5]

ZnO NPs also have potent antimicrobial, antibacterial, and ultraviolet (UV) inhibiting properties. ZnO NPs were successfully integrated into the textile sector, and the resulting fabrics exhibited UV and visible light resistance, antibacterial characteristics, and deodorant capabilities—all desired qualities.[6] So, more studies were anticipated into the use of ZnO NPs in antibacterial agents such as ointments, lotions, and mouthwashes. Coating various surfaces with it prevents germs from adhering, spreading, and reproducing on medical devices.[7]

Fixed retainer technology has a significant benefit over detachable retainer technique since it does not need patient cooperation; nevertheless, it does necessitate more thorough oral hygiene surrounding the retainers.[8] The most prevalent drawback is the increased risk of plaque and calculus buildup.[9]

Limited studies have looked at the antibacterial activity of titanium 6 aluminum 4 vanadium (Ti-6Al-4V) alloy, one of the materials used to make fixed orthodontic retainers.[10]

The goal of this study was to analyze in detail, via various characterization techniques and in vitro testing, the effect of ZnO NPs addition on Ti-6Al-4V alloy as substrate for fixed orthodontic retainer via the EPD process, specifically focusing on its surface and antibacterial properties.

The null hypothesis stated that coating Ti-6Al-4V alloy with ZnO NPs has no effect on the surface and antimicrobial characteristics.

Materials and Methods

Materials

The alloy used in the current study (►**Fig. 1**) was Ti-6Al-4V from Baoji Jinsheng Metal Material Co. Ltd (China) tested in Ministry of Science and Technology, Iraq. The percentages of titanium, aluminum, and vanadium were respectively 90, 6, and 4%.[11]

Methods

Sample Preparation

The Ti-6Al-4V alloy sheets were cut into small pieces with dimensions of $20 \times 10 \times 2$ mm for all tests (►**Fig. 2**). For antimicrobial tests, they were cut into disc shapes with a diameter of 6 mm and a thickness of 2 mm (►**Fig. 3**) using a DK7735 wire cutting machine (China) to prevent overheating.[12–14] The samples' surfaces were ground with silicon carbide papers to a 500-p finish, polished with a cloth and diamond paste, and cleaned in an ultrasonic bath for 15 minutes to remove any contaminants.[15]

Preparation of EPD Apparatus and Suspension of ZnO NPs

An EPD cell was created using a 100-mL beaker filled with a ZnO NPs suspension. The suspension was prepared by dissolving 1 g/L (1% volume) of polyvinylpyrrolidone in a mixture of 5% water and 94% ethanol.[16] The solution was stirred for 15 minutes at room temperature, followed by the addition of ZnO NP powder at concentrations of 2, 3, 4, and

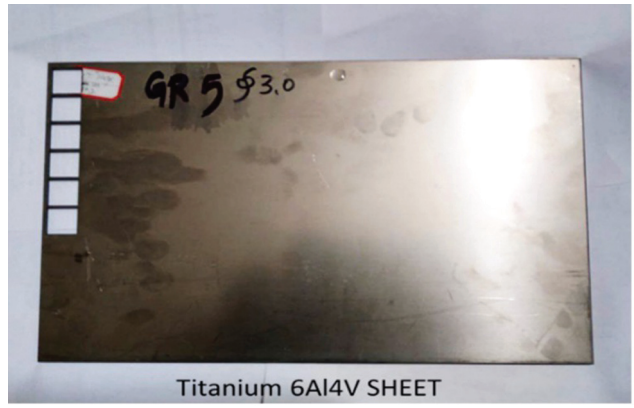

Fig. 1 Titanium 6 aluminum 4 vanadium (Ti-6Al-4V) alloy.

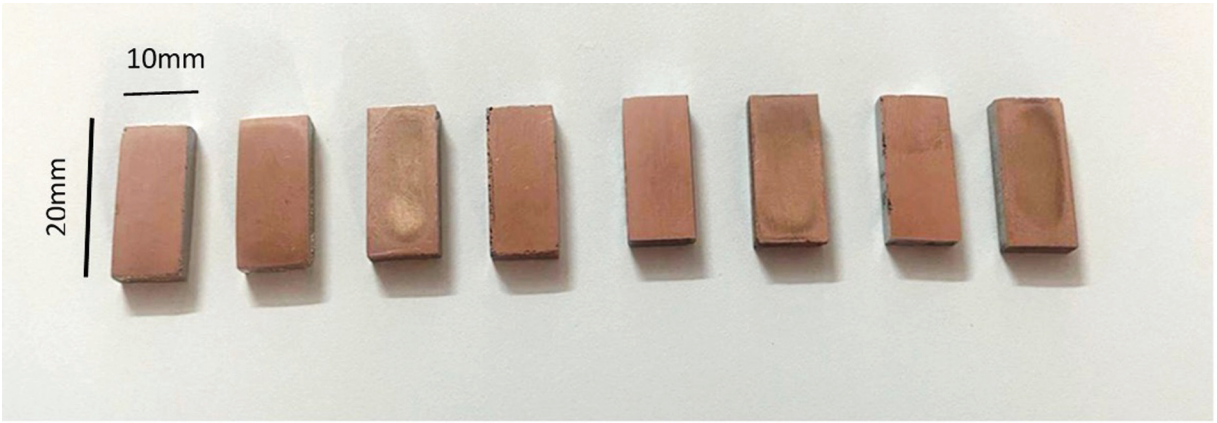

Fig. 2 Samples for electrophoretic deposition (EPD), titanium 6 aluminum 4 vanadium (Ti-6Al-4V) substrate (20 × 10 × 2 mm).

Fig. 3 Samples for antimicrobial test.

5 g/L.[17] The mixture was stirred for 6 hours and sonicated for 30 minutes to ensure uniform dispersion.[18]

The titanium alloy substrate served as the cathode, and graphite was used as the anode. The electrodes were submerged in the suspension, and the EPD process was carried out at varying voltages (10, 30, and 50 volts) and electrode distances (1, 3, and 5 cm) for each set of experiments. After deposition, the samples were air-dried and heat-treated at 150°C for 1 hour to enhance the adhesion of the ZnO coating.

Electrophoretic Deposition Technique

For EPD, three parameters were changed to achieve the optimized coating parameters. These parameters are the concentration of ZnO NPs, so 2, 3, 4, and 5 mg were used. The second parameter was the voltage and 10, 30, and 50 volts were used. The third parameter was the distance between the electrodes, and here 1, 3, and 5 cm were used, hence, nine specimens were prepared according to the parameters of optimization (►**Fig. 4**).

- 0 control samples have no coating
- 2 g/L concentration of ZnO NPs, 50 voltage and 1 cm distance between electrodes
- 3 g/L concentration of ZnO NPs, 50 voltage and 1 cm distance between electrodes
- 4 g/L concentration of ZnO NPs, 50 voltage and 1 cm distance between electrodes
- 5 g/L concentration of ZnO NPs, 50 voltage and 1 cm distance between electrodes
- 5 g/L concentration of ZnO NPs, 10 voltage and 1 cm distance between electrodes
- 5 g/L concentration of ZnO NPs, 30 voltage and 1 cm distance between electrodes

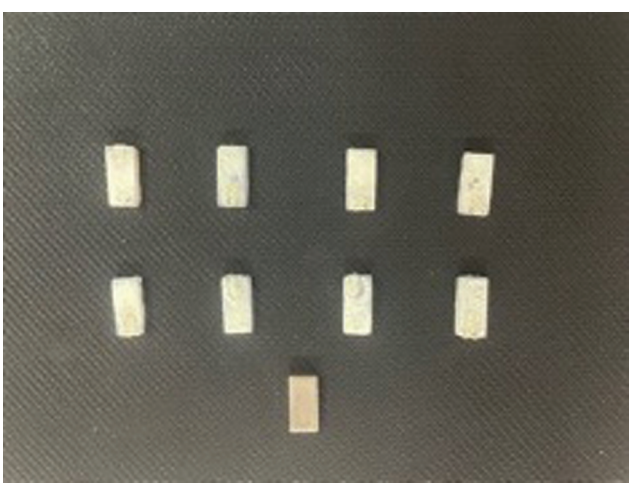

Fig. 4 The specimens for electrophoretic deposition.

- 5 g/L concentration of ZnO NPs, 50 voltage and 3 cm distance between electrodes
- 1 g/L concentration of ZnO NPs, 50 voltage and 5 cm distance between electrodes

X-Ray Diffractometer

The X-ray diffractometer (XRD) measuring machine is an apparatus qualified to characterize material's crystalline phases from single or complex composites. Its principle of action entails radiating the substrate surface with incident X-ray beams that collide with sample's atoms, then measuring the deflected X-rays angles and XRD analyses were performed using XRD (Model: XRD-6000 supplied with Cu, NF X-ray Tube and scanning radius of 185 mm). The leakage X-rays were less than 2.5 µSv/h at maximum out.

Atomic Force Microscope

Whether in air or liquid, atomic force microscopy (AFM) can characterize the three-dimensional structure of a wide range of materials, including conductors, insulators, inorganics, organics, biologicals, and so on. Due to its adaptability, AFM may be combined with other methods by using unique probes and gear. Accurate, high-resolution height measurements on the nanoscale are possible using AFM.[19] The morphology and roughness of coated sample surfaces were analyzed using AFM.[20] These tests were performed in College of Chemistry, University of Baghdad, Baghdad, Iraq, using NaioAFM apparatus (Switzerland). The NaioAFM is the ideal AFM for nano-education and basic research on small samples. This all-in-one AFM system provides solid performance and easy handling, with a price tag and footprint that fit anyone and any place.

Field Emission Scanning Electron Microscopy

The ultra-high resolution images captured by the field emission scanning electron microscopy (FE-SEM) need only modest accelerating voltages and short working distances. With the aim of providing a thorough assessment of specimens, FE-SEM is built on a technology for high-resolution imaging and several contrasting procedures. Imaging surface-sensitive and non-conductive samples is possible with FE-SEM without any preparatory steps.[21] FE-SEM used in this study was Inspect F50 from FFI company (Netherlands) at Al-Khora Lab, Baghdad, Iraq. The magnification used was up to 110,000× for 500 nm picture morphology.

Energy-Dispersive X-Ray Spectroscopy

An electron microscopy-related elemental analysis method, energy-dispersive X-ray spectroscopy (EDX) microanalysis works by producing distinctive X-rays that may be used to identify the elements present in a given material. EDX was used in order to determine the element composition that is present in the samples.[22] The device used in the current study was AxiaChemi SEM from Thermo Fisher Scientific Inc. (Netherlands).

Antimicrobial Test

Bacterial cultures of *Streptococcus mutans*, *Lactobacillus acidophilus*, and *Candida albicans* were grown in Brain Heart Infusion Broth. A suspension of each microorganism was prepared to a concentration of 10^7 colony-forming units per mL using a McFarland densitometer (0.5 McFarland standard).

The coated and uncoated specimens were autoclaved at 121°C for 20 minutes for sterilization. Sterile specimens were incubated in the bacterial suspensions for 24 hours at 37°C (►**Fig. 5A** and **B**). After incubation, the specimens were washed in phosphate-buffered saline to remove nonadherent cells and stained with 1% crystal violet for 10 minutes. Excess stain was washed off, and the specimens were immersed in 96% ethanol for 3 minutes to release the adhered dye (►**Fig. 5A–E**). The optical density (OD) of each sample was measured using a spectrophotometer (APEL PD-303, Japan) at 600 nm for bacteria and 540 nm for *C. albicans* as shown in ►**Fig. 6**.[23,24]

Statistical Analysis

Data of OD test were analyzed using SPSS software version 25. Descriptive statistics were represented by the means, standard deviations, minimum, and maximum values, while independent samples *t*-test was used for comparison between the groups for different microorganisms. The level of significance was set at 0.05.

Results

X-Ray Diffract Meter

To learn more about the crystallinity of the nanostructured ZnO-sensing film, an XRD analysis was performed. ►**Fig. 7** displayed the XRD pattern of the ZnO-nanostructured layer that was coated over the Ti-6Al-4V alloy substrate.

The XRD result showed a prominent (002) peak. The film's polycrystalline nature is shown by the sharp, strong peaks. The metallic layer below, identified by the (101) peak at 39.03 degrees, serves as an extended electrode and corresponds to Ti-6Al-4V alloy.

To determine the nanocrystallite size (L) using XRD radiation with wavelength λ (nm), the Scherrer equation was used. The XRD configuration of ZnO NPs coat for EPD method of coating is shown in ►**Fig. 7** for the three parameters of optimization. Two different 2θ peaks are related to Ti-6Al-4V substrate (35.094° (100), 38.422° (002)), for ZnO NPs 8 peaks appear (31.770° (100), 34.42° (002), 36.253° (101), 47.539° (102), 56.603° (110), 62.864° (103), 67.943° (112), 69.100° (201)) (International Centre for Diffraction Data 36-1451). The strong (002) peak shown in the XRD result corresponds to the hexagonal wurtzite structure with preferred orientation along the *c*-axis. The XRD pattern fairly matches with the Joint Committee on Powder Diffraction Standards (JCPDS) card. It is seen that the XRD patterns measured for the deposit prepared at 50 volts, 5 mg concentration, and 1 cm distance between the electrodes for 10 minutes showed strong diffraction lines of ZnO which is attributed to the amount of deposited ZnO increase almost linearly with the increase in concentration of nanosized ZnO. The average crystalline size for ZnO NPs coated by EPD is 38.14 nm.

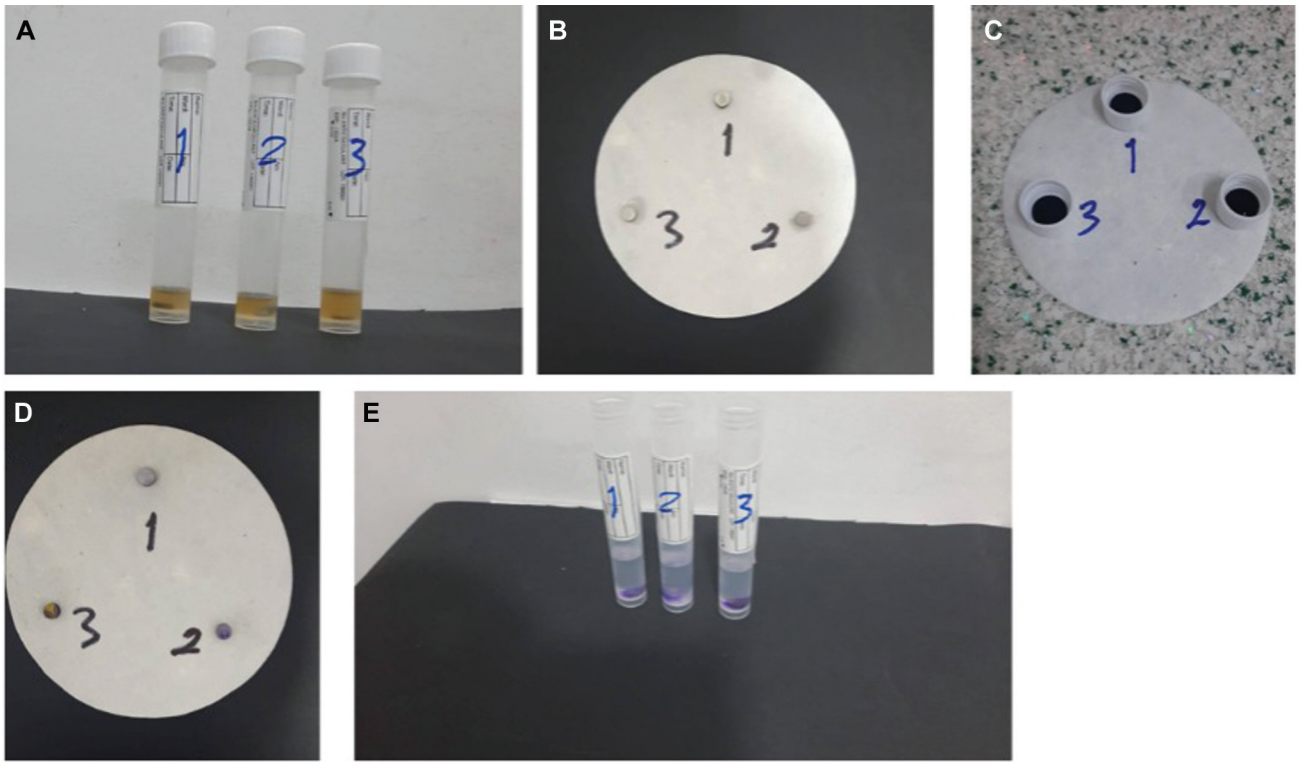

Fig. 5 Adherence test of bacteria and candida.

Fig. 6 (A) Vortex mixer, (B) spectrophotometer.

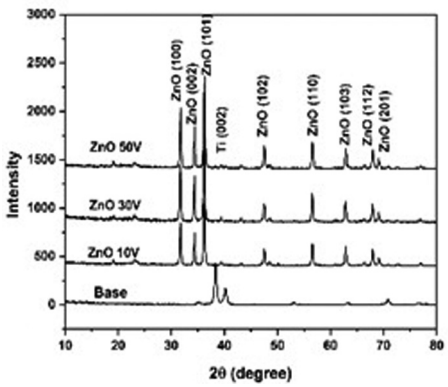

Fig. 7 X-ray diffractometer (XRD) pattern of samples.

Atomic Force Microscope

To analyze surface morphology, the 1 µm × 1 µm AFM images were acquired from the sample. ►**Fig. 8** displayed the typical grain size in two and three dimensions, as well as the typical sample diameter. This picture demonstrated a rather even distribution of ZnO NPs. For optimized sample the number of particles was 97, the root mean square height was 44.10 nm, the maximum height was 305.4 nm, arithmetic mean height was 35.48, and the mean diameter was 42.99.

Field Emission Scanning Electron Microscopy

ZnO NPs are studied by means of a FE-SEM to determine their structure, morphology, and size. FE-SEM is similar to SEM in many respects, with the primary difference being the use of a field emission electron source. When compared to SEM, which employs thermionic electron sources to produce electron beams, FE-SEM instead uses a potential gradient.

In the FE-SEM, the electron source is a field emission gun with a single tungsten filament that ends in a sharp point. The construction of an electron probe with a tip as tiny as 0.5 nm enabled imaging with more resolution than is possible with conventional SEM. In addition, better resolution surface topography pictures may be obtained with acceleration voltages as low as 5 kV. Claims have been made that by reducing the contact volume, resolution may reach 500 nm. The low-energy electron beam contributes to improved resolution and surface character by reducing the volume of interaction. ►**Fig. 9** depicts the surface morphology of a sample that has been optimally processed.

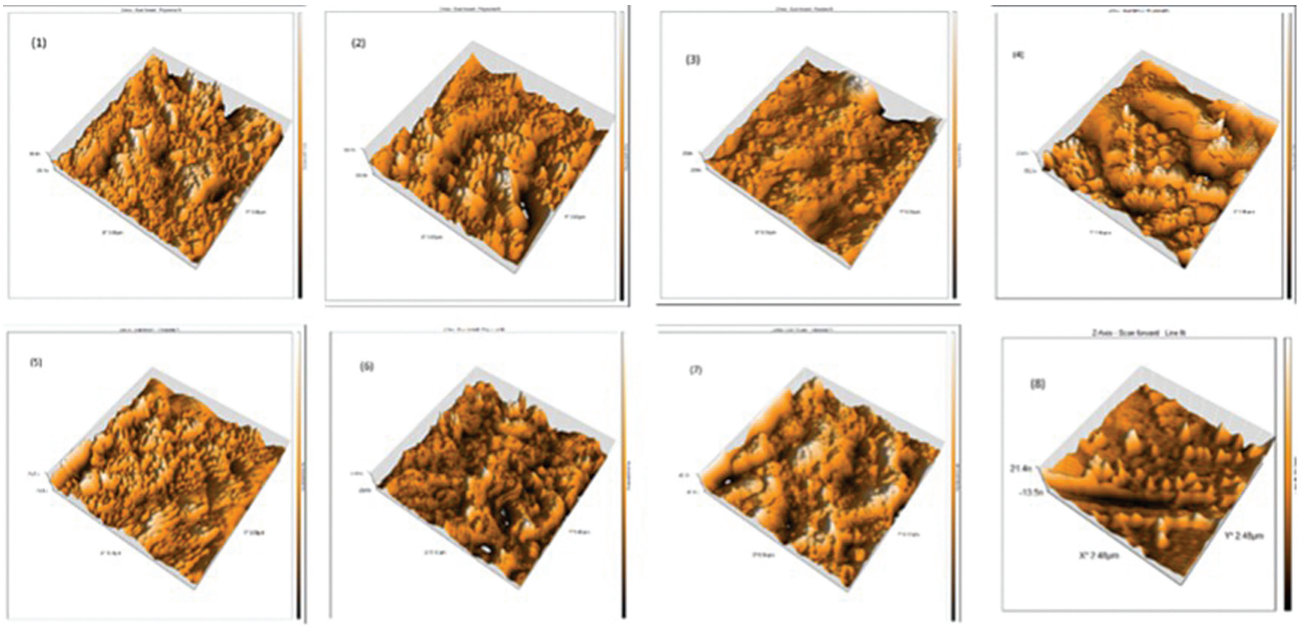

Fig. 8 Three dimension atomic force microscopy (AFM) scan.

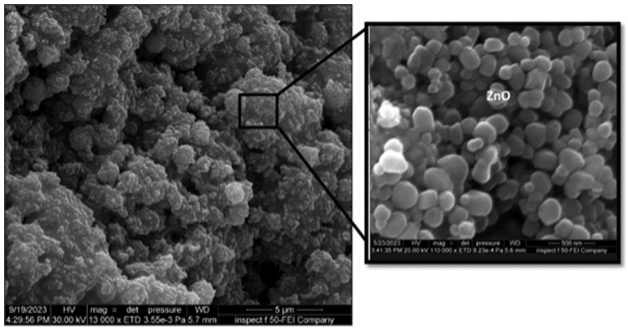

Fig. 9 110,000× magnification of zinc oxide nanoparticles (ZnO NPs) by field emission scanning electron microscopy (FE-SEM).

Energy-Dispersive X-Ray Spectroscopy

It additionally allows feasible image analysis and elemental mapping of a sample. Since the EDX analysis method does not require any sample preparation, it may be used to evaluate specimens of interest without causing any damage to them. Mapping of elements, dote, and EDX analysis of elements chart are presented in ►**Table 1** and ►**Figs. 10** and **11**.

Microbial Adherence Test (Optical Density)

After surface physical characteristics, the optimized sample with best surface morphology, lowest cracks, and homogenous coat layer was obtained and in the current research, this sample was the sample coat with parameters of optimization 5 g/L, 50 volt, and 1 cm distance between poles. Then, this optimized sample was prepared with the same parameter in number of 10 samples and subjected to antiadherence OD test against *S. mutans*, *L. acidophilus*, and *C. albicans* to compare their antiadherence effect with control (not coated samples).

The amount of light scattering brought on by bacteria in a culture is measured by OD. The more bacteria present, the more light is scattered. Since 600 nm is not hazardous to the culture, it is the wavelength that is specially selected for bacterial OD measurements in contrast to UV wave lengths. The 540-nm wavelength is specifically chosen for Candida OD measurements. ►**Table 2** and ►**Fig. 12** show the OD for *S. mutans*, Lactobacilli, and Candida, respectively. It is clear that the least amount of microbial adherence is shown in EPD-coated samples and the highest level of microbial adherence is shown in the control samples with a high significant difference ($p \leq 0.001$).

Discussion

This is the first study that investigated the effect of ZnO NPs coating the titanium orthodontic retainer substrate specifically the Ti-6Al-4V alloy using EPD technique and OD. Recently, the antimicrobial effect of ZnO NPs has been evaluated using the same method of coating but assessed with the inhibition zone method.[25] Previous study incorporated ZnO NPs to the orthodontic bonding agent.[26]

The quick forming time, straightforward equipment, and capacity to create uniform coatings on intricate geometries are benefits of the EPD technique. Furthermore, by simply altering deposition time and applied potential, EPD allows simple control over layer thickness and shape.[1]

The XRD analysis was performed for phase detection of NPs, in addition to the coated layer on substrate to verify that there was no phase transformation during the coating procedure.[27] A prominent 002 peak was shown and this is consistent with the wurtzite structure having a hexagonal shape and a *c*-axis orientation that is favored. The XRD pattern is consistent with the JCPDS card in size and shape.[28]

The film's polycrystalline nature is shown by the sharp, strong peaks. The metallic layer below, identified by the (101) peak at 39.03 degrees, serves as an extended electrode and corresponds to Ti-6Al-4V alloy.[29]

Table 1 EDX of optimized sample for Zn and O

Groups		Element	Atomic %	Atomic % error	Weight %	Weight % error
C	Control	Al	10.2	0.2	6.0	0.1
		Ti	85.7	0.6	89.5	0.6
		V	4.0	0.3	4.5	0.4
1	1 g, 50 v, 1 cm	O	66.0	0.9	32.2	0.4
		Zn	34.0	1.6	67.8	3.2
2	3 g, 50 v, 1 cm	O	83.9	1.1	56.1	0.7
		Zn	16.1	1.6	43.9	4.5
3	4 g, 50 v, 1 cm	O	74.0	1.2	41.0	0.7
		Zn	26.0	2.0	59.0	4.6
4	5 g, 50 v, 1 cm	O	68.3	0.4	34.5	0.2
		Zn	31.7	0.5	65.5	1.0
5	5 g, 10 v, 1 cm	O	75.1	0.9	42.5	0.5
		Zn	24.9	1.4	57.5	3.1
6	5 g, 30 v, 1 cm	O	81.0	1.0	51.0	0.6
		Zn	19.0	1.5	49.0	3.9
7	5 g, 50 v, 3 cm	O	71.1	0.7	37.5	0.4
		Zn	28.9	1.1	62.5	2.5
8	5 g, 50 v, 5 cm	O	63.7	0.9	30.1	0.4
		Zn	36.3	1.7	69.9	3.3

Abbreviations: Al, aluminum; EDX, energy-dispersive X-ray; Ti, titanium; V, vanadium; ZnO, zinc oxide.

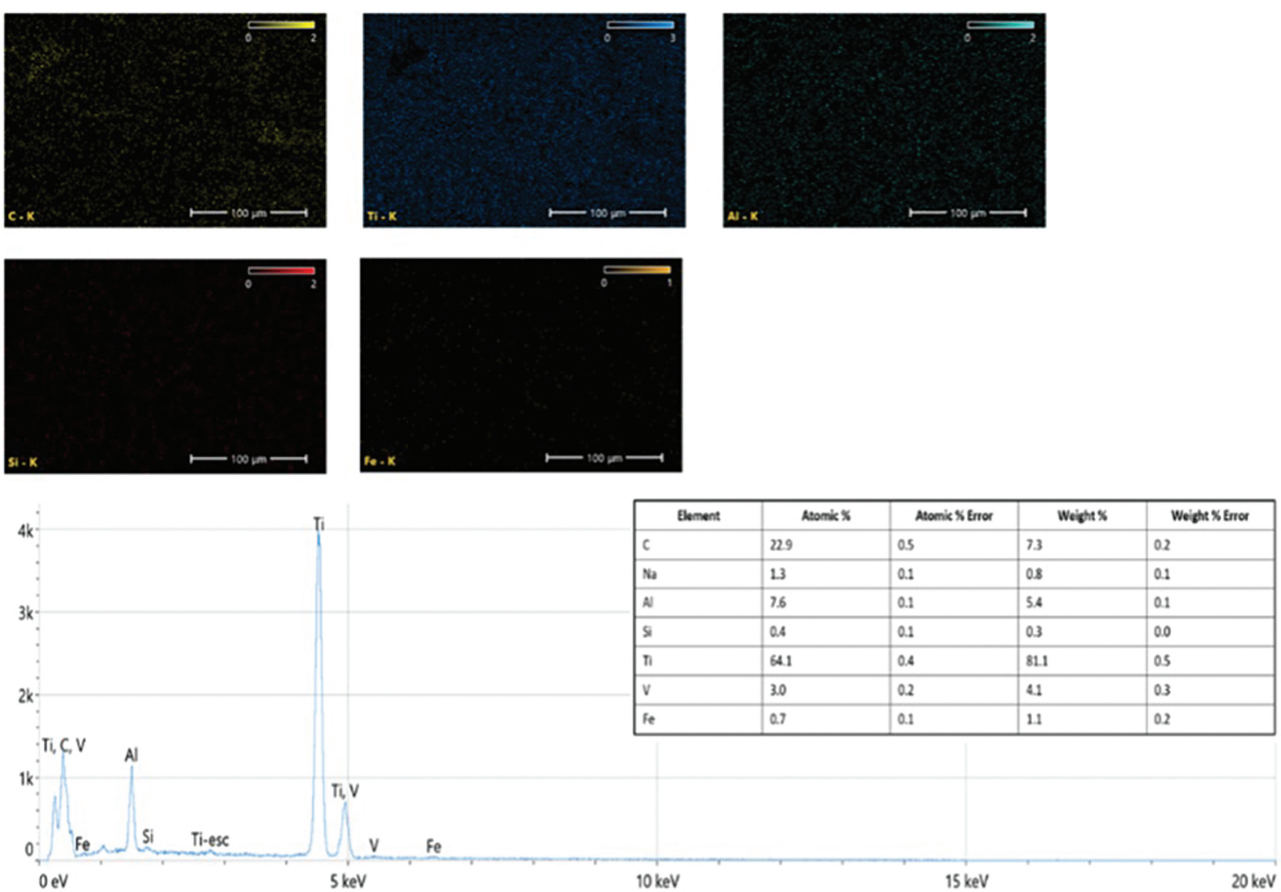

Fig. 10 Elemental analysis of titanium 6 aluminum 4 vanadium (Ti-6Al-4V) alloy (control).

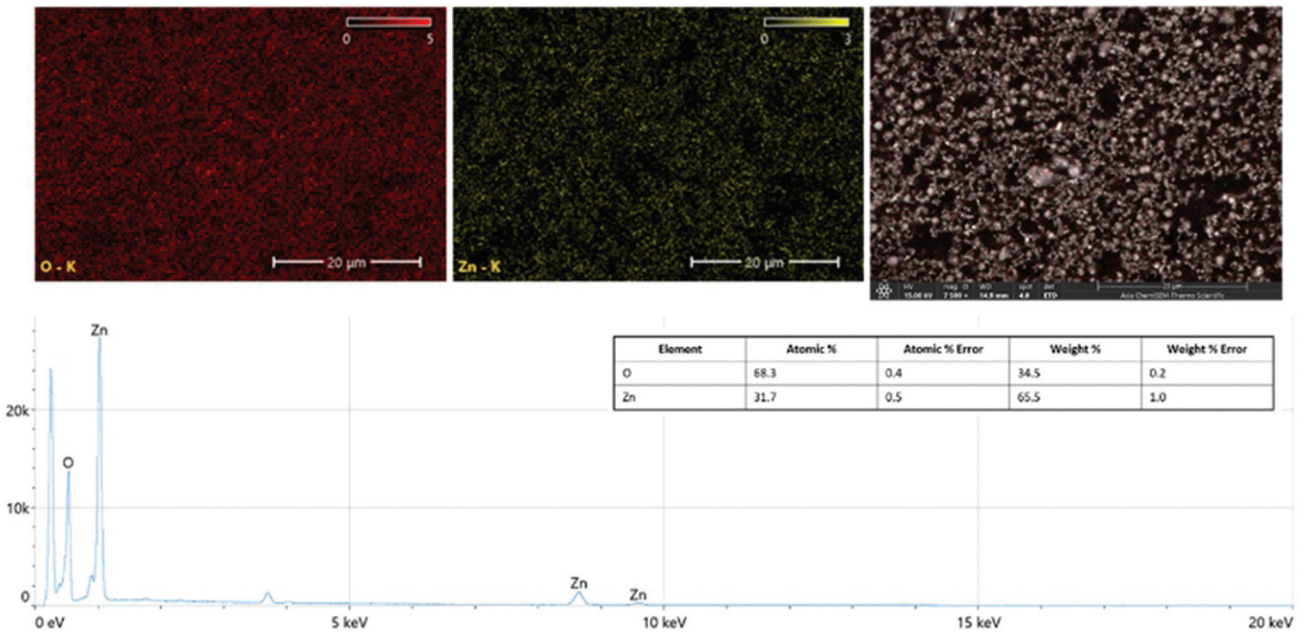

Fig. 11 Elemental analysis of the alloy coated by zinc oxide nanoparticles (ZnO NPs) by electrophoretic deposition (EPD) (5 g, 50 V, 1 cm).

The purpose of employing XRD radiation with a wavelength of λ (nm) is to find the nanocrystallite size (L), the Scherrer equation $L = K\lambda/\beta.\cos\theta$ was applied. This equation uses the entire width at half maximum of peaks (β) in radian measured at any two in the pattern to get the nanocrystallite size (L). *K*'s shape factor may range from 0.62 to 2.08, but is often estimated at 0.89.[30,31]

For the eight samples of EPD method, the average values of crystallite size were 29.4, 30.684, 32.14, 38.14, 31.83, 30.68, 30.86, and 32.96 nm. All crystallite sizes were in nanometer scales and in good range from the original particles size which was 30 nm. The largest one is the sample with highest voltage, highest concentration, and the smallest distance between poles. Modest applied fields (25–100 V/cm) result in more homogeneous film deposition, as stated by Basu et al,[32] while using comparatively larger applied fields (> 100 V/cm) results in a decline in film quality. The pace at which the particles accumulate affects how they pack themselves into the coating since the creation of the particulate film on the electrode is a kinetic phenomenon. This finding agrees with Humayun and Mills who found that a rise in voltage caused a rise in current flow, which in turn raised ionic concentration, which aided in the deposition of more metal, but they did not mention the effect on the crystallite size.[33]

It is also predicted that the ZnO-related peaks would be sharper relative to the background when the ZnO concentration of the composite samples is larger. The crack is increased with increase in voltage. In the present study, crack was very limited; this may be due to the heat treatment after deposition process and shrinkage. The crack is never seen in samples with 30 and 50 volt but the thickness is less in 30-volt samples and less corrosion resistance than samples with 50 volt. This finding is coinciding with the finding of Rahmadani et al[34] who found that coatings created at 30 volts showed stronger compaction and fewer flaws (pores and fractures) compared to samples made at 50 volt, making them more resistant to corrosion attack.

In this investigation, the 50-volt sample exhibited excellent homogeneous deposition. For biomedical applications, the ideal voltage for electroplating a ZnO coating at a thickness that is adequate for the coating's durability and

Table 2 Descriptive and comparative statistics of optical density of microorganisms (nm) between the groups

Microorganisms	Groups	Descriptive statistics				Comparison	
		Mean	SD	Min	Max	*t*-Test	*p*-Value
Streptococcus mutans	Control	0.094	0.00088	0.093	0.095	68.935	0.000
	EPD	0.061	0.00123	0.060	0.064		
Lactobacillus acidophilus	Control	0.101	0.00082	0.100	0.102	91.017	0.000
	EPD	0.056	0.00133	0.054	0.058		
Candida albicans	Control	0.098	0.00282	0.090	0.100	35.479	0.000
	EPD	0.062	0.00149	0.060	0.064		

Abbreviations: EDP, electrophoretic deposition; SD, standard deviation.

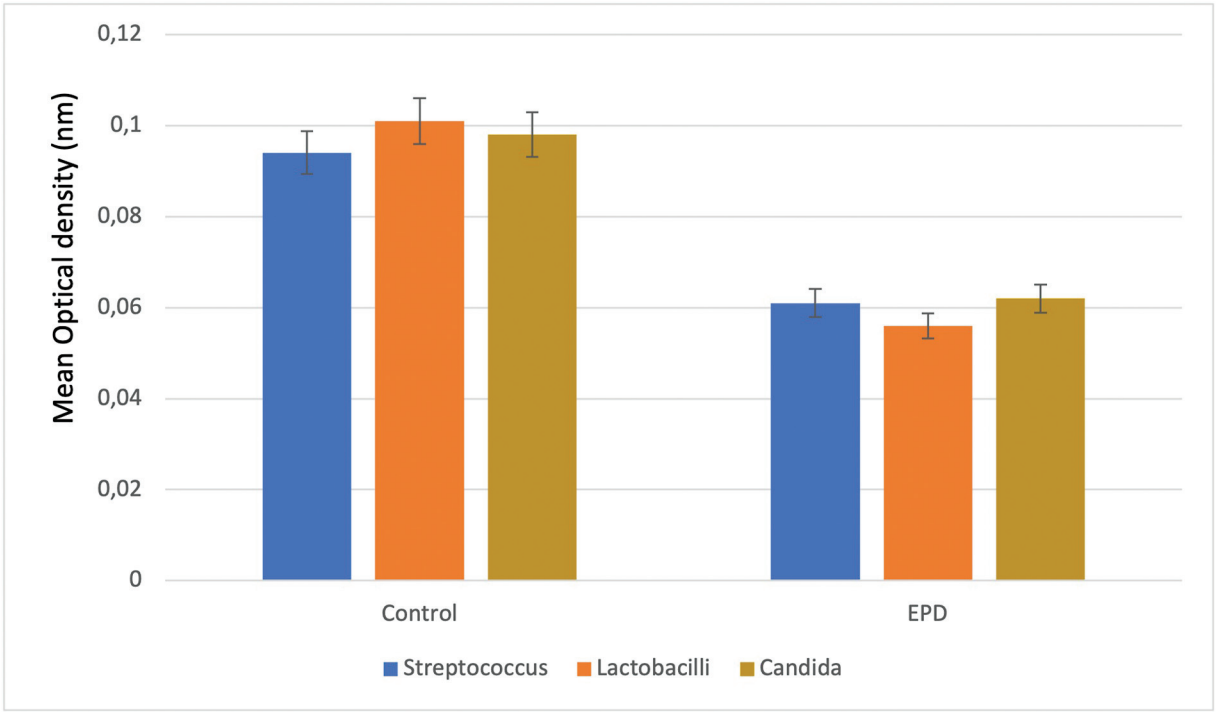

Fig. 12 Bar charts for the mean microbial adherence test using optical density.

strong resistance to electrochemical corrosion in physiological solutions was 50 volt.

The surface morphology of the ZnO NPs coat obtained from the AFM analysis showed good roughness. The average roughness of ZnO in this study is in agreement with the result obtained by Al-Ali et al.[35] The average particle size and morphology result from FE-SEM was in nanoscale and the surface texture was homogenous and consistent with the findings of Bahrami et al.[36]

Biofilms are clinically significant in the development of chronic and persistent infections. As a potential replacement agent for the treatment of biofilms and drug-resistant bacteria, ZnO NPs showed remarkable antibacterial and antibiofilm effectiveness against the biofilm-producing microorganisms.[25,37]

Size, lattice constant, and orientation are three variables that might impact ZnO's antibacterial activity; nevertheless, the most important of these is the V_O (oxygen vacancies), the physical and chemical characteristics of metal oxides, like ZnO, are greatly affected by oxygen vacancies, which are frequent native point defects surface concentration on ZnO.[38]

ZnO NPs-mediated suppression of bacterial growth could be linked to different mechanisms: The antibiofilm action of ZnO NPs is accounted for by their ability to disrupt the integrity of bacterial biofilms. ZnO NPs affect the production of exopolysaccharides, which are essential for the initial attachment of bacteria to host cells and the formation of complex biofilms. In addition, ZnO NPs were shown to have excellent penetrating and killing capabilities against bacterial cell walls.[39]

An innovative strategy for preventing biofilm development is to target the hydrophobicity of cell surfaces. In microbial interactions and biofilm structures, cell surface hydrophobicity and exopolysaccharide are key components. According to earlier research, one strategy to counteract biofilm creation in certain microbes is to interfere with the hydrophobicity of their cell surfaces. In addition, phagocytes and mucosal epithelial cells may be more attracted to bacterial cells due to their surface's enhanced hydrophobicity.[40]

However, ZnO NPs have an effect on gene expression that is implicated while dealing with oxidative stress and during the process of biofilm formation. Organisms that were exposed to ZnO NPs showed a considerable suppression of gene expression compared to untreated cells, including genes involved in biofilm formation oxidative stress (katA), interferon alpha and beta (icaA and sarA), and the overall regulator sigB. Reportedly, agr plays a pivotal role in controlling the initiation and progression of biofilms. Low agr transcription is required for biofilm development, adhesion, and maturation because its activation stimulates dispersion of bacterial cells to transition to a planktonic condition. Additionally, ZnO NPs inhibit the fibrillation of amyloid peptides, which is crucial for the development of bacterial biofilms.[41]

ZnO NPs have the potential to modify the expression of genes, particularly those linked to adhesion structures like fimbriae, pilus, or capsules[42] either extracellular matrix formation or quorum sensing. The adhesion and capsular encoding genes play a crucial role in the production of biofilms. ZnO NPs inhibit the expression of the capsular gene. Furthermore, ZnO NPs block genes linked to bacteria biofilm formation (like intercellular adhesion A, icaA) and quorum sensing (like accessory gene regulator, agr). Given that ZnO NPs have antibiofilm action.[43]

ZnO causes harm to bacteria and prevents the formation of biofilms by elevating oxygen-based reactive species, including free radicals, hydrogen peroxide, and hydroxyl

superoxide anion. These can result in the oxidative stress-induced destruction of cellular components, including proteins, lipids, and deoxyribonucleic acid.[44]

An additional process is the generation of Zn^{2+} ions during ZnO NPs dissolution. Zn^{2+} ions cause delay of bacterial growth and obstruct metabolic functions such quorum sensing, acid tolerance, glycolysis, and active and passive proton transfer across membranes. To get further insight into how ZnO NPs eradicate bacteria, these pathways are crucial.[45–57] When bacteria were grown using ZnO NPs, the production of bacterial biofilms was much decreased, as seen by confocal microscopy and crystal violet staining. Apart from their bactericidal properties, ZnO NPs may potentially disrupt cell-to-cell communication by modifying their surface negative charge or zeta potential, hence preventing substrate surface attachment. According to the previous findings, the null hypothesis was rejected.

Strengths

1. Because titanium alloy has good biocompatibility, it is utilized extensively in dentistry. Applying a ZnO NPs coating enhances its antibacterial properties while maintaining its biocompatibility.
2. To maximize their antibacterial effect, ZnO NPs may be produced in a variety of sizes and morphologies. Because of its adaptability, it may be customized for a certain application and its intended microorganisms.
3. The effectiveness of ZnO NPs as an antibacterial is already well supported by science. This body of research gives confidence in this strategy's ability to avoid infections related to medical alloys.

Clinical Implications

Testing ZnO NPs coatings' antibacterial activity on titanium alloy has intriguing therapeutic implications since it may lower infection rates, increase patient safety, lengthen implant life, and promote technological and medical practice developments.

Limitations

Using Ti-6Al-4V alloy substrate (instead of retainer wire) and performing the study in vitro may be considered as the major limitations of this study.

Future Perspectives

1. Performing investigations to evaluate ZnO NPs coatings' long-term stability and durability on titanium alloy surfaces. Examine how effectively the coating maintains its antimicrobial qualities over time, taking biological interactions, wear, and corrosion into account.
2. Starting clinical studies to assess the efficacy and safety of titanium retainers coated with ZnO NPs in human patients to determine clinical viability, evaluate patient outcomes, success rates, and infection rates over long periods of time.
3. Attempting to create standardized processes for coating titanium alloys with ZnO NPs verifying that medical device regulations are being followed.

Conclusion

The EPD is an effective and inexpensive method of coating orthodontic titanium retainer substrate. The samples are affected by different parameters of coating but the optimized sample with good physical properties is that with the highest concentration used (5 g), highest voltage, and minimum distance between poles. The antimicrobial efficiency of Ti-6Al-4V was enhanced by coating with ZnO NPs.

Authors' Contributions
Conceptualization: S.A.M., M.N.; methodology: M.K.K., M.N., S.A.M.; software: S.A.M., M.N.; formal analysis: S.A.M., M.N.; investigation: S.A.M., M.N.; data curation: M.N., S.A.M.; writing—original draft preparation: S.H., M.C., G.M.; writing—review and editing: M.C., G.M.; supervision: G.M.; funding acquisition: S.H.; administration: S.H. All authors have read and agreed to the published version of the manuscript.

Funding
None.

Conflict of Interest
None declared.

Acknowledgment
None.

References

1 Morrison FA Jr, Stukel JJ. Electrophoresis of an insulating sphere normal to a conducting plane. J Colloid Interface Sci 1970;33(01):88–93
2 Fotovvati B, Namdari N, Dehghanghadikolaei A. On coating techniques for surface protection: a review. J Manuf Mater Process 2019;3(01):28
3 Mishra PK, Mishra H, Ekielski A, Talegaonkar S, Vaidya B. Zinc oxide nanoparticles: a promising nanomaterial for biomedical applications. Drug Discov Today 2017;22(12):1825–1834
4 Minervini G, Franco R, Marrapodi MM, Almeida LE, Ronsivalle V, Cicciù M. Prevalence of temporomandibular disorders (TMD) in obesity patients: A systematic review and meta-analysis. J Oral Rehabil 2023;50(12):1544–1553
5 Minervini G, Franco R, Marrapodi MM, Di Blasio M, Isola G, Cicciù M. Conservative treatment of temporomandibular joint condylar fractures: A systematic review conducted according to PRISMA guidelines and the Cochrane Handbook for Systematic Reviews of Interventions. J Oral Rehabil 2023;50(09):886–893
6 Hatamie A, Khan A, Golabi M, et al. Zinc oxide nanostructure-modified textile and its application to biosensing, photocatalysis, and as antibacterial material. Langmuir 2015;31(39):10913–10921
7 Jiang J, Pi J, Cai J. The advancing of zinc oxide nanoparticles for biomedical applications. Bioinorg Chem Appl 2018;2018:1062562
8 Årtun J. Caries and periodontal reactions associated with long-term use of different types of bonded lingual retainers. Am J Orthod 1984;86(02):112–118
9 Al Groosh DH, Bozec L, Pratten J, Hunt NP. The influence of surface roughness and surface dynamics on the attachment of Methicillin-resistant Staphylococcus aureus onto orthodontic retainer materials. Dent Mater J 2015;34(05):585–594
10 Pesode PA, Barve SB. Recent advances on the antibacterial coating on titanium implant by micro-Arc oxidation process. Mater Today Proc 2021;47(16):5652–5662

11 Rack HJ, Qazi JI. Titanium alloys for biomedical applications. Mater Sci Eng C 2006;26(08):1269–1277
12 Hadzhieva Z, Boccaccini AR. Recent developments in electrophoretic deposition (EPD) of antibacterial coatings for biomedical applications - a review. Curr Opin Biomed Eng 2022;21:100367
13 Minervini G, Franco R, Marrapodi MM, Fiorillo L, Cervino G, Cicciù M. Post-traumatic stress, prevalence of temporomandibular disorders in war veterans: Systematic review with meta-analysis. J Oral Rehabil 2023;50(10):1101–1109
14 Minervini G, Franco R, Marrapodi MM, Fiorillo L, Cervino G, Cicciù M. The association between parent education level, oral health, and oral-related sleep disturbance. An observational crosssectional study. Eur J Paediatr Dent 2023;24(03):218–223
15 Kaya S, Boccaccini AR. Electrophoretic deposition of zein coatings. J Coat Technol Res 2017;14:683–689
16 Koczkur KM, Mourdikoudis S, Polavarapu L, Skrabalak SE. Polyvinylpyrrolidone (PVP) in nanoparticle synthesis. Dalton Trans 2015;44(41):17883–17905
17 Abdulhussein DA. An antimicrobial nanoparticles coated fixed orthodontic retainer (An in vitro study). PhD thesis, University of Baghdad; 2022
18 Cordero-Arias L, Cabanas-Polo S, Gao H, et al. Electrophoretic deposition of nanostructured-TiO_2/chitosan composite coatings on stainless steel. RSC Adv 2013;3(28):11247–11254
19 Klapetek P, Valtr M, Nečas D, Salyk O, Dzik P. Atomic force microscopy analysis of nanoparticles in non-ideal conditions. Nanoscale Res Lett 2011;6(01):514
20 Kadhim MJ, Abdulateef NE, Abdulkareem MH. Evaluation of surface roughness of 316L stainless steel substrate on nanohydroxyapatite by electrophoretic deposition. Al-Nahrain J Engineering Sci 2018;21(01):28–35
21 Cik RC, Foo CT, Nor AF. Field Emission Scanning Electron Microscope (FESEM) Facility in BTI. NTC 2015: Nuclear Technical Convention 2015, Malaysia
22 Scimeca M, Bischetti S, Lamsira HK, Bonfiglio R, Bonanno E. Energy dispersive X-ray (EDX) microanalysis: a powerful tool in biomedical research and diagnosis. Eur J Histochem 2018;62(01):2841
23 Xu P, Yang H, Tian L, et al. Function and safety evaluation of Staphylococcus epidermidis with high esterase activity isolated from strong flavor Daqu. Lebensm Wiss Technol 2023;176;114534
24 Kareem YM, Hamad TI. Assessment of the antibacterial effect of Barium Titanate nanoparticles against *Staphylococcus epidermidis* adhesion after addition to maxillofacial silicone. F1000 Res 2023;12:385
25 Mohammed SA, Nahidh M, Khalaf MK. Synthesis and antibacterial activity of ZnO nanoparticle coatings for titanium orthodontic fixed retainers. J Nanostructures 2023;13(04):978–988
26 Hailan SY, Al-Khatieeb MM. Antimicrobial efficacy of silver, zinc oxide, and titanium dioxide nanoparticles incorporated in orthodontic bonding agent. J Bagh Coll Dent 2019;31(03):10–16
27 Arefi MR, Rezaei-Zarchi S. Synthesis of zinc oxide nanoparticles and their effect on the compressive strength and setting time of self-compacted concrete paste as cementitious composites. Int J Mol Sci 2012;13(04):4340–4350
28 Rajendran SP, Sengodan K. Synthesis and characterization of zinc oxide and iron oxide nanoparticles using Sesbania grandiflora leaf extract as reducing agent. J Nanosci 2017;2017:1–17
29 Hadimani RL. Rare-Earth magnetocaloric thin films. In: El-Gendy AA, Barandiarán JM, Hadimani RL, eds. Magnetic Nanostructured Materials. 1st ed. Cambridge: Elsevier; 2018:269–294
30 Monshi A, Foroughi MR, Monshi MR. Modified Scherrer equation to estimate more accurately nano-crystallite size using XRD. World J Nano Sci Engineering 2012;2(03):154–160
31 Turky RN, Jassim RK. The electrophoretic deposition of nano Al_2O_3 and $AgNO_3$ on CpTi dental implant: an in-vitro and in-vivo study. J Bagh Coll Dent 2016;28(01):41–47
32 Basu RN, Randall CA, Mayo MJ. Fabrication of dense zirconia electrolyte films for tubular solid oxide fuel cells by electrophoretic deposition. J Am Ceram Soc 2001;84(01):33–40
33 Humayun A, Mills D. Voltage regulated electrophoretic deposition of silver nanoparticles on halloysite nanotubes. Results Mater 2020;7:100112
34 Rahmadani S, Anawati A, Gumelar MD, Hanaf R, Jujur IN. Optimizing parameter for electrophoretic deposition of hydroxyapatite coating with superior corrosion resistance on pure titanium. Mater Res Express 2022;9(11):115402
35 Al-Ali DA, Al Groosh D, Abdulkareem MH. The influence of Chitosan on adhesion of silver oxide nanoparticles coating on SS 316L in biomedical applications. J Res Med Dent Sci 2022;10 (03):195–200
36 Bahrami R, Pourhajibagher M, Badiei A, Masaeli R, Tanbakuchi B. Evaluation of the cell viability and antimicrobial effects of orthodontic bands coated with silver or zinc oxide nanoparticles: an *in vitro* study. Korean J Orthod 2023;53(01):16–25
37 Agrawal A, Sharma R, Sharma A, et al. Antibacterial and antibiofilm efficacy of green synthesized ZnO nanoparticles using Saraca asoca leaves. Environ Sci Pollut Res Int 2023;30(36): 86328–86337
38 Bruna T, Maldonado-Bravo F, Jara P, Caro N. Silver nanoparticles and their antibacterial applications. Int J Mol Sci 2021;22(13):7202
39 Mahamuni-Badiger PP, Patil PM, Badiger MV, et al. Biofilm formation to inhibition: role of zinc oxide-based nanoparticles. Mater Sci Eng C Mater Bio Appl 2020;108:110319
40 Kuttinath S, Sevanan M, Rammohan R. Inhibition of Methicillin resistant Staphylococcus aureus biofilm by ethanol extracts of Sauropus androgynus and Solanum torvum. Indian J Pharm Sci 2021;83(06):1155–1163
41 Abdelghafar A, Yousef N, Askoura M. Zinc oxide nanoparticles reduce biofilm formation, synergize antibiotics action and attenuate Staphylococcus aureus virulence in host; an important message to clinicians. BMC Microbiol 2022;22(01):244
42 Ghasemian A, Mobarez AM, Peerayeh SN, Bezmin Abadi AT. The association of surface adhesin genes and the biofilm formation among *Klebsiella oxytoca* clinical isolates. New Microbes New Infect 2018;27:36–39
43 Bianchini Fulindi R, Domingues Rodrigues J, Lemos Barbosa TW, et al. Zinc-based nanoparticles reduce bacterial biofilm formation. Microbiol Spectr 2023;11(02):e0483122
44 Prema D, Binu NM, Prakash J, Venkatasubbu GD. Photo induced mechanistic activity of GO/Zn(Cu)O nanocomposite against infectious pathogens: Potential application in wound healing. Photodiagnosis Photodyn Ther 2021;34:102291
45 Rosenberg M, Visnapuu M, Vija H, et al. Selective antibiofilm properties and biocompatibility of nano-ZnO and nano-ZnO/Ag coated surfaces. Sci Rep 2020;10(01):13478
46 Toti Ç, Kaçani G, Meto A, et al. Early treatment of class II division 1 malocclusions with prefabricated myofunctional appliances: a case report. Prosthesis 2023;5(04):1049–1059
47 Karakas-Stupar I, Zaugg LK, Zitzmann NU, Joda T, Wolfart S, Tuna T. Clinical protocol for implant-assisted partial removable dental prostheses in Kennedy class I: a case report. Prosthesis 2023;5 (04):1002–1010. Doi: 10.3390/prosthesis5040069
48 Cumbo E, Messina P, Gallina G, Scardina GA. An experimental method to add new prosthetic teeth in the removable partial denture framework: TIG cold welding and preformed pins. Prosthesis 2023;5(04):1120–1128
49 Alkahtany M, Beatty MW, Alsalleeh F, et al. Color stability, physical properties and antifungal effects of ZrO_2 additions to experimental maxillofacial silicones: comparisons with TiO_2. Prosthesis 2023;5(03):916–938
50 Maniaci A, La Mantia I, Mayo-Yáñez M, et al. Vocal rehabilitation and quality of life after total laryngectomy: state-of-the-art and systematic review. Prosthesis 2023;5(03):587–601
51 Carossa M, Scotti N, Alovisi M, et al. Management of a malpractice dental implant case in a patient with history of oral bisphosphonates intake: a case report and narrative review of recent findings. Prosthesis 2023;5(03):826–839

52 Al Ramil AM, Lamfoon S, Mawardi H. Dental implants for patients with oral mucosal diseases: a narrative review and clinical guidance. Dent Med Probl 2023;60(04):687–696
53 Bommala M, Koduganti RR, Panthula VR, et al. Efficacy of root coverage with the use of the conventional versus laser-assisted flap technique with platelet-rich fibrin in class I and class II gingival recession: a randomized clinical trial. Dent Med Probl 2023;60(04):583–592
54 Inchingolo AD, Ceci S, Patano A, et al. Elastodontic therapy of hyperdivergent class II patients using AMCOP® devices: a retrospective study. Appl Sci (Basel) 2022;12(07):3259
55 Inchingolo AD, Malcangi G, Semjonova A, et al. Oralbiotica/oralbiotics: the impact of oral microbiota on dental health and demineralization: a systematic review of the literature. Children (Basel) 2022;9(07):1014. Doi: 10.3390/children9071014
56 Bollero P, Arcuri L, Miranda M, Ottria L, Franco R, Barlattani A Jr. Marfan syndrome: oral implication and management. Oral Implantol (Rome) 2017;10(02):87–96
57 Franco R, Gianfreda F, Miranda M, Barlattani A, Bollero P. The hemostatic properties of chitosan in oral surgery. Biomed Biotechnol Res J 2020;4(03):186